

# Is Room Temperature Superconductivity in Carbon Nanotubes Too Wonderful to Believe?

Guo-meng Zhao\*

Department of Physics and Astronomy,  
California State University at Los Angeles,  
Los Angeles, CA 90032, USA

**ABSTRACT:** It is well known that copper-based perovskite oxides rightly enjoy consensus as high-temperature superconductors on the basis of two signatures: Meissner effect and zero resistance. In contrast, I provide over twenty signatures for room temperature superconductivity in carbon nanotubes. The one-dimensionality of the nanotubes complicates the right-of-passage for prospective quasi-one-dimensional superconductors. The Meissner effect is less visible because the diameters of nanotubes are much smaller than the penetration depth. Zero resistance is less obvious because of the quantum contact resistance and significant quantum phase slip, both of which are associated with a finite number of transverse conduction channels. Nonetheless, on-tube resistance at room temperature has been found to be indistinguishable from zero for many individual multi-walled nanotubes. On the basis of more than twenty arguments, I suggest that carbon nanotubes deserve to be classified as room temperature superconductors. The mechanism for room-temperature superconductivity may arise from strong electron-phonon and electron-plasmon coupling.

**Key words:** Room-temperature superconductivity, carbon nanotubes

## 1 Introduction

Finding room temperature (RT) superconductors is one of the most challenging problems in science. It was theoretically shown that RT superconductivity cannot be realized within the conventional phonon-mediated pairing mechanism [1]. It has also been demonstrated that a polaronic effect can enhance superconductivity substantially [2]. But it is unclear whether RT superconductivity can be achieved within this mechanism. On the other hand, a theoretical calculation showed that superconductivity as high as 500 K can be reached through a pairing interaction mediated by undamped acoustic plasmon modes in a quasi-one-dimensional electronic system [3]. Moreover, high-temperature superconductivity can occur in a multi-layer electronic system due to an attraction of charge carriers in the same conducting layer via exchange of virtual plasmons in neighboring layers [4]. If these theoretical studies are relevant, one should be able to find high-temperature superconductivity in quasi-one-dimensional (1D) and/or multi-layer systems.

Carbon nanotubes constitute a novel class of quasi-one-dimensional materials which would offer the potential for high-temperature superconductivity. The simplest single-

walled nanotube (SWNT) consists of a single graphite sheet which is curved into a long cylinder, with a diameter which can be smaller than 1 nm. Band-structure calculations predict that carbon nanotubes have two types of electronic structures depending on the chirality [5, 6], which is indexed by a chiral vector  $(n, m)$ :  $n - m = 3N + \nu$ , where  $N, n, m$  are the integers, and  $\nu = 0, \pm 1$ . The tubes with  $\nu = 0$  are metallic while the tubes with  $\nu = \pm 1$  are semiconductive. Multiwalled nanotubes (MWNTs) consist of at least two concentric shells which could have different chiralities. The MWNTs possess both quasi-one-dimensional and multi-layer electronic structures. This unique quasi-one-dimensional electronic structure in both SWNTs and MWNTs makes them ideal for plasmon-mediated high-temperature superconductivity.

In a series of five papers [7, 8, 9, 10, 11] resident on the cond-mat e-print archive since November 2001, I provide over twenty arguments for RT superconductivity in carbon nanotubes. In this article, I will review some of these arguments and provide more evidence for room-temperature superconductivity in carbon nanotubes.

## 2 Electrical transport and tunneling spectra in SWNTs

It is well known that, for quasi-1D systems disorder has extremely strong effects on electrical transport [12, 13]. For a noninteracting 1D system, all states get localized in the presence of an infinitesimal random potential [14]. Interactions can modify this picture, as shown clearly from theoretical studies of one-chain and two-chain systems using bosonization and renormalization-group techniques [12, 13]. It is shown that metal-like conductivity occurs only for strongly attractive interactions that lead to quasi-1D s-wave high-temperature superconductivity [12, 13]. In contrast, for repulsive interactions d-wave superconductivity would occur for the pure system and, in the presence of disorder and/or impurities, the resistivity is found to decrease monotonically with increasing temperature even at high temperatures (semiconductor-like behavior) [13]. Thus, d-wave superconductivity and a normal-state Luttinger liquid are not compatible with a metal-like resistivity in quasi-1D systems [13].

Alternatively, the metal-like conductivity below a mean-field superconducting transition temperature  $T_{c0}$  in quasi-1D s-wave superconductors can be understood in terms of quantum phase slips (QPS). Indeed, QPS theories [15, 16] can well explain a number of experiments that show a large resistance and its metal-like temperature dependence well below  $T_{c0}$  in thin superconducting wires [15, 17, 18, 19].

Essentially, the phase slips at low temperatures are related to the macroscopic quantum tunneling (MQT), which allows the phase of the superconducting order parameter to fluctuate between zero and  $2\pi$  at some points along the wire, resulting in voltage pulses. The QPS tunneling rate is proportional to  $\exp(-S_{QPS})$ , where  $S_{QPS}$  in clean superconductors is very close to the number of transverse channels  $N_{ch}$  in the limit of weak damping (see below). If the number of transverse channels  $N_{ch}$  is small, the QPS tunneling rate is not negligible, leading to a non-zero resistance at low temperatures. For a SWNT,  $N_{ch} = 2$ , implying a large QPS tunneling rate and thus a finite resistance even if it is a superconductor. For MWNTs with several superconducting layers adjacent to each other,  $N_{ch}$  will increase substantially, resulting in the large suppression of the QPS if the Josephson coupling among the layers is strong. If two superconducting tubes are closely packed together to effectively increase  $N_{ch}$ , one would find a substantially reduced on-tube resistance at RT if the constituent tubes have a mean-field  $T_{c0}$  well above RT.

There are thermally activated phase slips (TAPS) and QPS in thin superconducting wires. TAPS occur via thermal activation and are dominant only at temperatures

slightly below and close to  $T_{c0}$ . At low temperatures, QPS dominate. The resistance at low temperature for carbon nanotubes due to MQT is shown to be [9]

$$R_{MQT} = \beta_1 \frac{h}{4e^2} \frac{L}{\xi} \sqrt{0.26\beta_2 N_m} \exp(-0.26\beta_2 N_m), \quad (1)$$

where  $L$  is the length of the wire,  $\xi$  is the coherence length,  $N_m$  is the number of metallic chirality shells,  $\beta_1$  and  $\beta_2$  are constants, depending on the damping strength. When the damping increases,  $\beta_2$  decreases.

In the limit of weak damping,  $\beta_2 = 7.2$  (Ref. [15]). Therefore, from Eq. 1 one can see that  $S_{QPS} \simeq 2N_m$ . For stronger damping,  $\beta_2$  is reduced so that  $S_{QPS} < 2N_m$ . Moreover, in the dirty limit,  $S_{QPS}$  will be further reduced [16] such that  $S_{QPS} \ll 2N_m$ . For a SWNT,  $N_m = 1$  so that a large QPS and a nonzero resistance is expected below  $T_{c0}$ . If several superconducting SWNTs are closely packed to ensure an increase in  $N_{ch}$ , the QPS would be substantially reduced. This can explain why for a single SWNT the on-tube resistance is appreciable at RT [20, 21] while for a bundle consisting of two strongly coupled SWNTs the RT resistance is very small [22]. For a MWNT with  $d = 40$  nm, a total of 27 transverse channels has been seen [23]. This implies that the QPS in this single MWNT should be strongly suppressed. Indeed, this MWNT has nearly zero on-tube resistance at RT over a length of 4  $\mu\text{m}$  (Ref. [23]).

A more rigorous approach quantifying the QPS in quasi-1D superconductors [16] suggests that  $S_{QPS}$  depends not only on  $N_{ch}$  but also on the normal-state conductivity  $\sigma$  ( $S_{QPS} \propto \sigma^{2/3}$ ). Therefore, one can effectively suppress the QPS and the resistance below  $T_{c0}$  by reducing the normal-state resistivity.

Within the QPS theory [16], the on-tube resistance  $R_i \propto T^{2\mu-3}$  for  $k_B T \gg \Phi_0 I/c$ , and  $R_i$  becomes independent of temperature and is proportional to  $I^{2\mu-3}$  for  $k_B T \ll \Phi_0 I/c$ . Here  $\Phi_0$  is the quantum flux,  $c$  is the speed of light,  $I$  is the current, and  $\mu$  is a quantity that characterizes the ground state. The zero-temperature resistance can approach zero when  $\mu > 2$ , but is finite when  $\mu \leq 2$ . When  $\mu < 1.5$ ,  $R_i$  increases with decreasing temperature (semiconducting behavior), while for  $\mu > 1.5$ ,  $R_i$  decreases with decreasing temperature (metallic behavior). Only if the QPS are strongly suppressed, can zero on-tube resistance be approached below  $T_{c0}$ .

For  $\Phi_0 I/c k_B \ll T \ll T_{c0}$ , the four-probe or two-probe resistance of a superconducting wire is given by

$$R(T) = R_0 + aT^p. \quad (2)$$

Here  $p = 2\mu - 3$ ,  $R_0 = R_Q/tN_{ch}$  for four-probe measurements,  $R_0 = R_Q/tN_{ch} + 2R_c$  for two-probe measurements,  $t$  is the transmission coefficient ( $t \leq 1$ ),  $R_Q = h/2e^2 = 12.9$  k $\Omega$  is the resistance quantum, and  $R_c$  is the contact resistance.

Now we compare the QPS theory with the resistance data of SWNTs that are known to exhibit quasi-1D superconductivity. For the smallest diameter SWNTs with  $d = 0.42$  nm,  $T_{c0}$  was found to be about 15 K [24]. In Fig. 1a, we plot the two-probe resistance as a function of  $T/T_{c0}$  for this SWNT. It is apparent that the resistance increases more rapidly above  $0.5T_{c0}$  and flattens out towards  $T_{c0}$ . From Fig. 1a, we also see that the normal-state resistance  $R_N$  at  $T_{c0}$  is larger than the zero-temperature resistance  $R_0$  by a factor of 34. Since  $R_0 \geq R_Q/N_{ch}$ , then  $R_N \geq 34R_Q/N_{ch}$ . With  $N_{ch} = 8$  per tube (Ref. [10]), we obtain  $R_N \geq 34R_Q/8 = 55$  k $\Omega$ . Because the contact distance is about 50 nm [24], the normal-state resistance per tube per unit length is larger than 1100 k $\Omega/\mu\text{m}$ . This suggests a very short mean free path ( $< 15$  Å) that makes ballistic transport impossible.

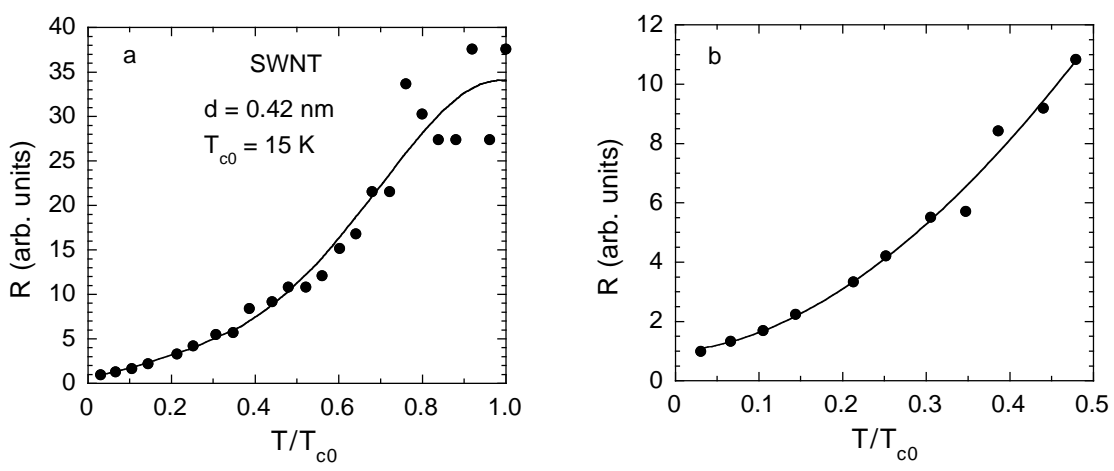


Figure 1: a) The resistance as a function of  $T/T_{c0}$  for the smallest diameter SWNTs with  $d = 0.42$  nm. The data are extracted from Ref. [24]. b) The temperature dependence of the resistance below  $0.5T_{c0}$ .

As demonstrated in Fig. 1b, below  $0.5T_{c0}$  the temperature dependence of the resistance can be well fitted by Eq. 2. From the fit, we find that  $p = 1.77 \pm 0.18$ . This suggests that the QPS theory can indeed explain the quasi-1D superconductivity in SWNTs. Using  $p = 1.77$  and  $p = 2\mu - 3$ , we obtain  $\mu = 2.4 > 2$ , implying zero on-tube resistance at zero temperature.

In Fig. 2a, we plot the temperature dependence of the resistance for a single SWNT. It is interesting that the temperature dependence of the resistance in this SWNT is similar to that found for ultrathin wires of MoGe superconductors [19], a facsimile of which is reproduced in Fig. 2b. By comparing Fig. 2a and Fig. 2b, one might infer that the mean-field  $T_{c0}$  of this nanotube is well above 270 K.

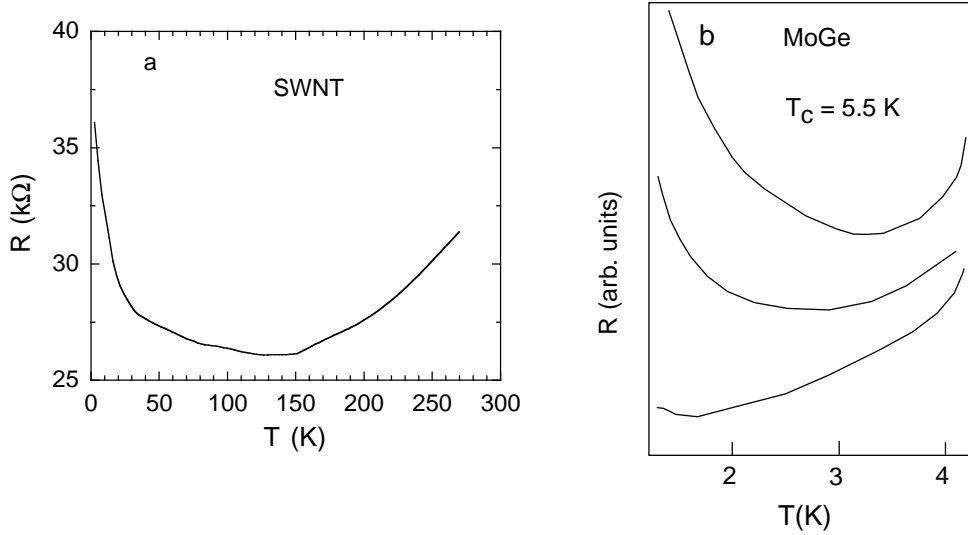


Figure 2: a) Temperature dependence of the resistance for a SWNT. The data are extracted from Ref.[20]. b) Temperature dependence of the resistance for three ultrathin MoGe wires. The curves are smoothed from the original plot of Ref. [19].

We can fit the data of Fig. 2a above a resistance-minimum temperature ( $\sim 150$  K) with Eq. 2. This will result in  $p > 1$ , which is inconsistent with electrical transport for a Luttinger liquid (LL). Phonon backscattering and/or electron umklapp scattering in a LL lead to a semiconductor-like resistivity at low temperatures and a power-law resistivity with  $p \simeq 0.6$  at high temperatures [25, 26]. Disorder gives rise to a high-

temperature power-law resistivity with  $p \simeq -0.4$  (Ref. [26]). Any combinations of these power laws predicted from the LL are not compatible with the data shown in Fig. 2a. Further, recent tunneling experiments have excluded LL behavior [27]. Moreover, the data in Fig. 2a also rule out quasi-1D d-wave superconductivity because quasi-1D d-wave superconductors behave like insulators at any temperatures [13].

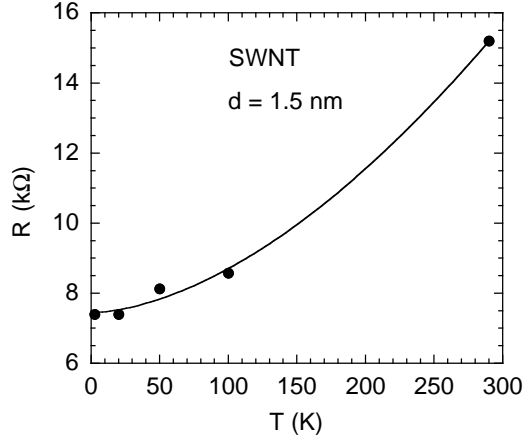


Figure 3: Temperature dependence of the resistance at zero gate voltage for a single-walled nanotube with  $d = 1.5$  nm. The data are extracted from Fig. 1a of Ref. [28].

Fig. 3 shows the temperature dependence of the resistance at zero gate voltage for a single-walled nanotube with  $d = 1.5$  nm. The distance between the two contacts is about 200 nm and the contacts are nearly ideal with the transmission probability of about 1 [28]. It is remarkable that the temperature dependence of the resistance can be fitted by Eq. 2 with  $p = 1.71 \pm 0.23$ . This exponent is very close to the one found for the smallest SWNTs with  $T_{c0} = 15$  K (see Fig. 1b). Further, the on-tube resistance at zero temperature is found to be nearly zero [28]. These results can be only explained by the QPS theory [16]. Using  $p = 1.71$  and  $p = 2\mu - 3$ , we get  $\mu = 2.35 > 2$ . This implies a negligible on-tube resistance at zero temperature according to the QPS theory [16], in agreement with experiment [28].

For a longer tube where the distance between the two contacts is about 800 nm, the resistance at zero gate voltage is independent of temperature below 270 K (Ref. [28]), i.e.,  $p \simeq 0$ . It was also shown that [28] underdoping leads to  $p < 0$  while overdoping gives rise to  $p > 0$ . This doping dependence of  $p$  is only consistent with the QPS theory. Within the QPS theory [16],  $\mu \propto r/\lambda_L \propto \sqrt{n}$  (where  $\lambda_L$  is the London penetration depth and  $n$  is the carrier density). It is clear that  $\mu$  increases with  $n$  such that  $p$  can cross over from a negative value at low doping to a positive one at high doping, in agreement with experiment [28].

Now we discuss tunneling spectra. From a single-particle tunneling spectrum obtained through two high-resistance contacts (see Fig. 1b of Ref. [21]), we can clearly see a pseudo-gap feature which appears at an energy of about 220 meV. The pseudo-gap feature could be related to the superconducting gap. Considering the broadening of the gap feature due to large QPS and the double tunneling junctions in series, we estimate the superconducting gap  $\Delta(0)$  to be about 100 meV. The scanning tunneling microscopy and spectroscopy [29] on individual single-walled nanotubes also show pseudo-gap features with  $\Delta(0) \simeq 100$  meV in doped metallic SWNTs. Using  $k_B T_{c0} = \Delta(0)/1.76$ , we find  $T_{c0} \simeq 660$  K.

This gap value deduced from the tunneling spectrum is in good agreement with electrical transport data for a SWNT rope (see Fig. 4). Below 200 K the resistivity is nearly temperature independent while above 200 K the resistivity increases suddenly

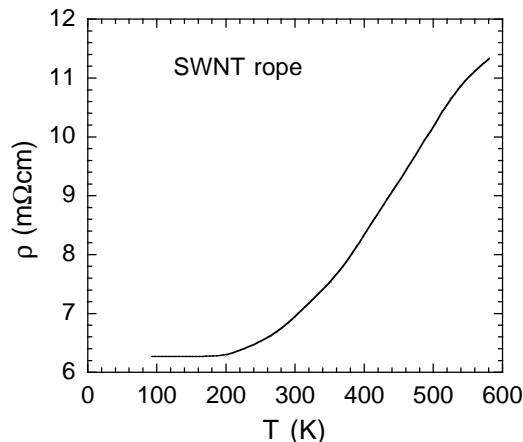


Figure 4: Temperature dependence of the resistivity for a SWNT rope with  $T_{c0} \simeq 640$  K. The data are extracted from Ref. [30].

and starts to flatten out above 550 K. By comparing with Fig. 1a, we find that this temperature dependence of the resistance agrees with quasi-1D superconductivity with a  $T_{c0} \simeq 640$  K. If we assume that one-third of the tubes have metallic chiralities (MC) and exhibit superconductivity and that the on-tube resistance is negligible below 200 K, we find that the normal-state on-tube resistivity for the MC tubes is about 1.6 mΩcm.

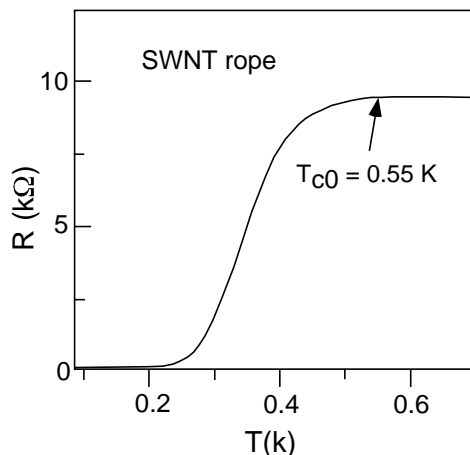


Figure 5: The temperature dependence of the resistance for a SWNT rope with  $T_{c0} = 0.55$  K. The figure is reproduced from Ref. [32]

The electrical transport and single-particle tunneling spectra thus consistently suggest that  $T_{c0}$  in SWNTs can be higher than 500 K. Nevertheless, a much lower  $T_{c0}$  was observed in a SWNT rope [32]. Fig. 5 shows temperature dependence of the resistance for the SWNT rope. One can see that the resistance starts to drop below about 0.55 K. The data agree with quasi-1D superconductivity with  $T_{c0} \simeq 0.55$  K. It is remarkable that the relative transition width  $\Delta T/T_{c0}$  for this SWNT rope is similar to that for another SWNT rope with  $T_{c0} \simeq 640$  K (see Fig. 4). With  $R_0 = 74 \Omega$  and assuming perfect contacts, one finds [32] that the normal-state resistance per tube per unit length is  $830 \text{ k}\Omega/\mu\text{m}$  which corresponds to the normal-state resistivity of  $128 \mu\Omega\text{cm}$  and a mean free path of  $78 \text{ \AA}$ . We should mention that very low superconductivity in this SWNT rope may be due to the fact that the tubes are very lightly doped. This is in agreement with the tunneling spectrum which shows no pseudo-gap feature at 5 K in an undoped or very lightly doped armchair tube [33]. The strong doping dependence of  $T_{c0}$  is consistent with the superconducting mechanism based on electron-plasmon

### 3 Raman scattering in a SWNT rope

It is known that Raman scattering has provided essential information about the electron-phonon coupling and the electronic pair excitation energy in the high- $T_c$  cuprate superconductors [35, 36, 37]. The anomalous temperature-dependent broadening of the Raman active  $B_{1g}$ -like mode of 90 K superconductors  $\text{RBa}_2\text{Cu}_3\text{O}_{7-y}$  (R is a rare-earth element) allows one to precisely determine the superconducting gap [36]. The pronounced softening observed only for the  $B_{1g}$  mode is due to the fact that the phonon energy of the  $B_{1g}$  mode is very close to  $2\Delta(0)$  and the mode is strongly coupled to electrons [36, 38].

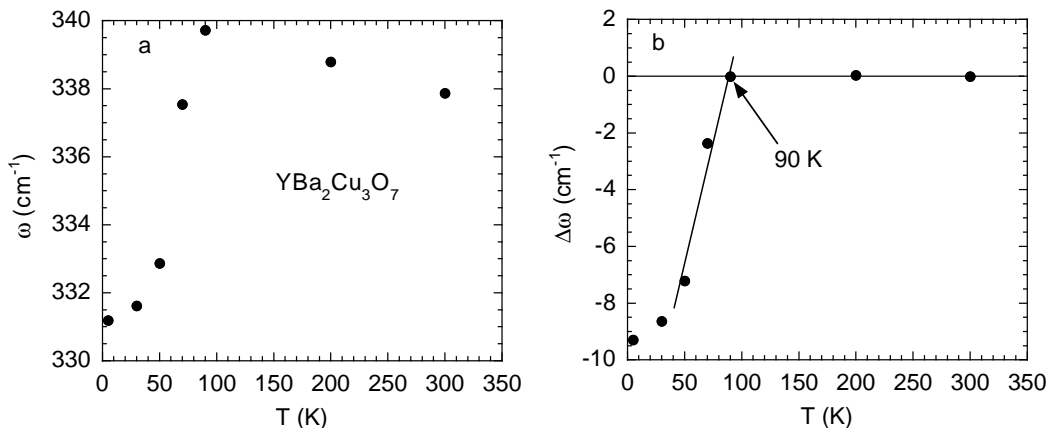


Figure 6: a) Temperature dependence of the frequency for the Raman-active  $B_{1g}$  mode of a 90 K superconductor  $\text{YBa}_2\text{Cu}_3\text{O}_{7-y}$ . The data are extracted from Ref.[35]. b) The difference between the measured frequency and the linearly fitted curve above  $T_c$ .

The temperature dependence of the frequency for the Raman-active  $B_{1g}$  mode of a 90 K superconductor  $\text{YBa}_2\text{Cu}_3\text{O}_{7-y}$  is shown in Fig. 6a. It is apparent that the frequency decreases linearly with increasing temperature above  $T_c$  and that the mode starts to soften below about  $0.95T_c$ . The temperature dependence of the frequency above  $T_c$  is caused by thermal expansion. The temperature dependence of the frequency will become more pronounced at higher temperatures since the magnitude of the slope  $-d \ln \omega / dT$  is essentially proportional to the lattice heat capacity that increases monotonically with temperature. The significant softening of the mode below  $T_c$  occurs only if the energy of the Raman mode is very close to  $2\Delta(0)$  and the electron-phonon coupling is substantial [38], as it is the case in the 90 K superconductor  $\text{YBa}_2\text{Cu}_3\text{O}_{7-y}$  [35, 36, 37]. In order to see more clearly the softening of the mode, we show in Fig. 1b the difference of the measured frequency and the linearly fitted curve above  $T_c$ . It is clear that the softening starts at about  $89 \text{ K} \simeq 0.95T_c$ .

Fig. 7a shows the temperature dependence of the frequency for the Raman active  $G$ -band of a SWNT rope. It is remarkable that the frequency data show a clear tendency of softening below about 630 K. Above 630 K, the frequency decreases linearly with increasing temperature, which is similar to the behavior in  $\text{YBa}_2\text{Cu}_3\text{O}_{7-y}$  (Fig. 6a).

In order to see more clearly the softening of the mode, we show in Fig. 7b the difference between the measured frequency and the linearly fitted curve above the kink temperature ( $\sim 630 \text{ K}$ ). It is striking that the result shown in Fig. 7b is similar to that shown in Fig. 6b. This suggests that the softening of the Raman active  $G$ -band in the SWNTs may have the same microscopic origin as the softening of the Raman active  $B_{1g}$

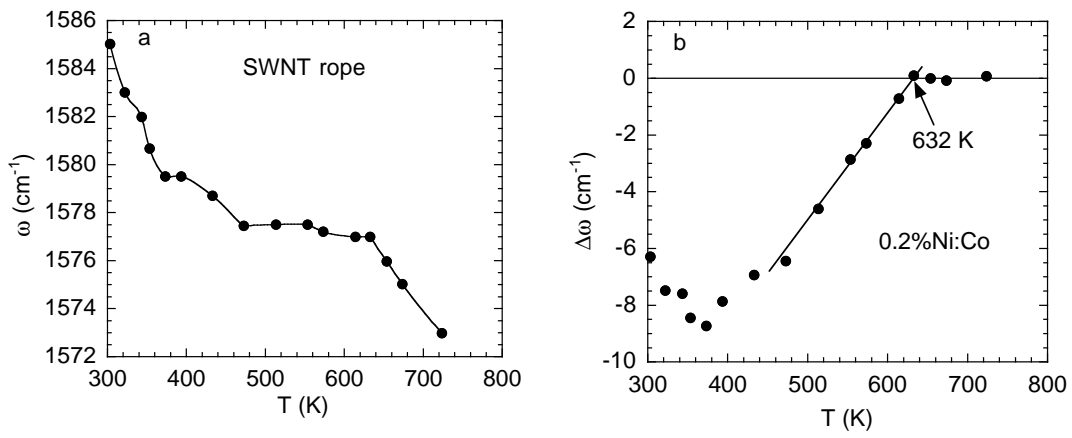


Figure 7: a) Temperature dependence of the frequency for the Raman active  $G$ -band of a SWNT rope. The data are from Ref. [34]. b) The difference of the measured frequency and the linearly fitted curve above the kink temperatures (see text).

mode in  $\text{YBa}_2\text{Cu}_3\text{O}_{7-y}$ . This explanation is plausible only if the phonon energy of the  $G$ -band is very close to  $2\Delta(0)$ . We are fortunate that the phonon energy of the  $G$ -band is 197 meV, very close to  $2\Delta(0) = 200$  meV deduced from the tunneling spectrum and the electrical transport experiment [9]. Therefore, it is very likely that the softening of the Raman mode in the SWNTs is related to a superconducting phase transition.

From Fig. 7, we can clearly see that the softening starts at about 632 K. Using the fact that the softening starts at  $0.95T_{c0}$  (Ref. [38]), we can assign the mean-field transition temperature  $T_{c0} = 665$  K.

It is interesting to note that there is a clear minimum at  $T^* = 370$  K  $= 0.57T_{c0}$  in Fig. 7b. It is remarkable that such a minimum is also seen at about  $0.6T_{c0}$  in a calculated curve for a superconductor (see Fig. 8 of Ref. [38]). This shallow minimum in the frequency shift is related to a sharp minimum in the real part of the polarization  $\Pi(\omega, T)$ , which occurs at  $\hbar\omega/2\Delta(T^*) = 1$  for weak coupling [38, 39]. This quantitative consistency provides strong evidence that the softening of the Raman active mode in the SWNTs is indeed associated with a superconducting phase transition.

From the temperature dependence of the BCS gap [40], we find that  $\Delta(T^*) = \Delta(0.57T_{c0}) = 0.93\Delta(0)$ . Using  $\hbar\omega/2\Delta(T^*) = 1$  and  $\hbar\omega = 197$  meV, we finally obtain  $\Delta(0) = 105$  meV, which is in excellent agreement with the value deduced from the tunneling spectrum [9]. Then we calculate  $2\Delta(0)/k_B T_{c0} = 3.66$ , which is very close to that expected from the weak-coupling BCS theory. This value is also in excellent agreement with the prediction based on the plasmon-mediated pairing mechanism [3].

#### 4 Electrical transport and tunneling spectrum in MWNTs

Subtle evidence for superconductivity above RT can be found in MWNT ropes [7]. Further, a negligible on-tube resistance ( $\sim 86 \Omega/\mu\text{m}$ ) has been observed at RT in the majority of individual MWNTs [41, 42]. If we use the average diameter of 15 nm for the MWNTs, we find that the average room-temperature resistivity is  $1.5 \mu\Omega\text{cm}$ , which is about three orders of magnitude smaller than the normal state resistivity for SWNTs. In order to explain such a small on-tube resistivity at RT, one must assume that these MWNTs have  $T_{c0}$ 's much higher than 300 K and QPS are significantly suppressed.

In Fig. 8, we show the magnetic field dependence of the resistivity at 298 K for a MWNT rope. For our MWNT ropes, we find that the average weight density is about 40% of the microscopic weight density ( $2.17 \text{ g/cm}^3$ ) [44]. The resistivity is calculated

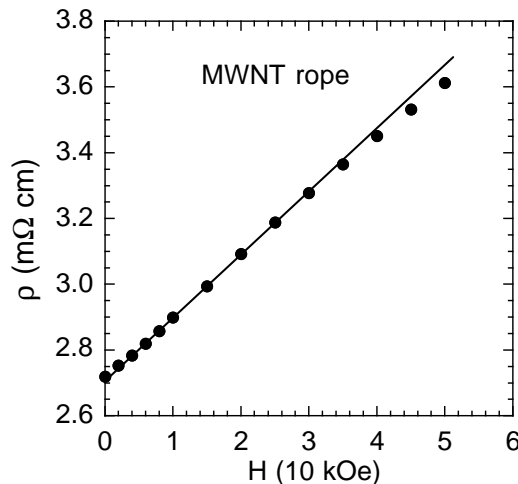


Figure 8: The magnetic field dependence of the resistivity at 298 K for a MWNT rope.

with this porosity correction. From Fig. 8, we can clearly see that the zero-field resistivity for the rope is about three orders of magnitude larger than the on-tube resistivity. This suggests that the room-temperature resistivity for this rope is dominated by the contact resistivity between tubes. Since there should be no magnetoresistance (MR) effect for the contact resistance, the result shown in Fig. 8 implies a very large on-tube MR effect, i.e.,  $\Delta\rho_i/\rho_i \simeq 60000\%$  at  $H = 50$  kOe (using  $\rho_i = 1.5 \mu\Omega\text{cm}$ ). Such a huge on-tube MR effect is hard to explain without invoking superconductivity.

Since there is a negligible positive MR effect for physically separated MWNTs up to 180 K (Ref. [45]), the observed large positive MR effect in physically coupled MWNT rope may be associated with the coupling of the tubes. However, no positive MR is observed up to 225 K for physically coupled SWNT ropes [46]. This suggests that the tube coupling alone is not sufficient to produce a huge positive MR effect. It is clear that the combined results cannot be explained if MWNTs were not RT superconductors. It is well known that the motion of vortices in a vortex-liquid state can cause resistivity that is proportional to the magnetic field [40]. When the sizes of all individual MWNTs are not large enough to trap any vortices [47], there will be no positive MR effect. This can account for the negligible positive MR effect for physically separated MWNTs. When individual MWNTs are closely packed into bundles, the sizes of Josephson coupled bundles are large enough to trap vortices so that a large positive MR can be observed in the vortex-liquid state, in agreement with the result shown in Fig. 8. No positive MR effect in physically coupled SWNT ropes suggests that the SWNTs are either nonsuperconducting or the sizes of Josephson coupled superconducting bundles are not large enough to trap any vortices.

If the positive MR effect is indeed caused by RT superconductivity, the normal-state resistivity at room-temperature should be larger than  $\rho(50\text{kOe}) - \rho(0) = 0.9 \text{ m}\Omega\text{cm}$  (see Fig. 8). This is because the resistivity is not completely saturated at  $H = 50$  kOe. This normal-state resistivity appears to be similar to the one for a SWNT rope ( $\sim 1.6 \text{ m}\Omega\text{cm}$ ). From the field dependence of the resistivity (see Fig. 8), one can also see that the melting field at room-temperature is very small.

In Fig. 9 we plot the temperature dependence of the resistance for a single MWNT with  $d \simeq 12$  nm. The contact distance is  $0.5 \mu\text{m}$ . It is striking that the temperature dependence of the resistance for this MWNT is similar to that (see Fig. 5) for a SWNT rope consisting of about 90 superconducting SWNTs. Below 200 K, the resistance is nearly temperature independent, which suggests that the on-tube resistance may be negligible below 200 K. By comparing Fig. 9 with Fig. 5, we may infer that  $T_{c0}$

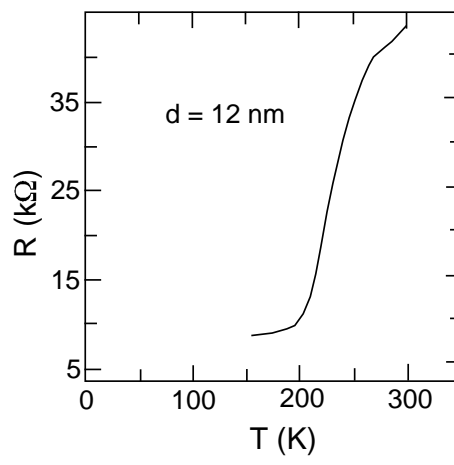


Figure 9: The temperature dependence of the resistance for a single MWNT with  $d \simeq 12$  nm, which is reproduced from Ref. [43]. The data are consistent with quasi-1D superconductivity with  $T_{c0} \simeq 400$  K.

$\simeq 400$  K. Assuming zero on-tube resistance below 200 K, we find that the normal-state resistance per unit length at 400 K is about  $66 \text{ k}\Omega/\mu\text{m}$ . This corresponds to the normal-state resistivity of  $0.75 \text{ m}\Omega\text{cm}$ . This normal-state resistivity is very close to that deduced from Fig. 8 ( $\geq 0.9 \text{ m}\Omega\text{cm}$ ), and also agrees with the value ( $1.6 \text{ m}\Omega\text{cm}$ ) for a SWNT rope (see Fig. 4).

From Fig. 9, we also see negligible on-tube resistance below  $200 \text{ K} \simeq 0.5T_{c0}$  for this individual MWNT. By analogy, the negligible on-tube resistance at RT observed in the majority of MWNTs [42] indicates that most MWNTs have  $T_{c0}$ 's higher than 600 K in agreement with the high-temperature resistance data [7].

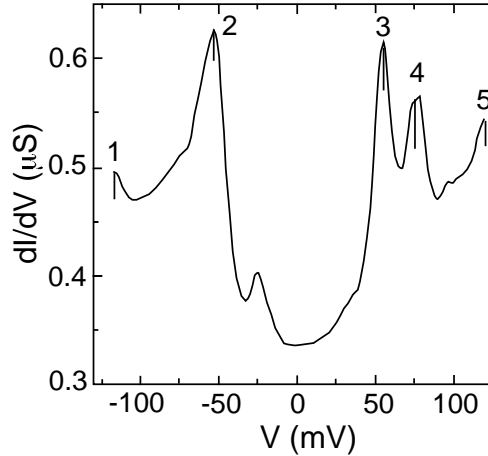


Figure 10: Single-particle tunneling spectrum for a single MWNT with  $d \simeq 17$  nm, which is reproduced from Ref. [48].

Fig. 10 shows single-particle tunneling spectrum for a single MWNT with  $d = 17$  nm. It is apparent that both the intensity and the peak position in this spectrum are inconsistent with the normal-state density of states for any types of metallic-chirality tubes [49, 50]. On the other hand, this spectrum is very similar to the one for a superconductor with a superconducting gap of about 54.4 meV. This gap size corresponds to  $T_{c0} = 360$  K according to the BCS relation.

We can quantitatively explain this spectrum by invoking superconductivity. The peak positions denoted by 1, 2, 3, 4, 5 are located at  $< -117 \text{ mV}$ ,  $-54.4 \text{ mV}$ ,  $54.4 \text{ mV}$ ,  $76.5 \text{ mV}$ , and  $\sim 120 \text{ mV}$ , respectively. Below  $T_{c0}$ , the Van Hove singularities are located

at  $E_{VH} = \pm\sqrt{[\Delta(0)]^2 + (\epsilon_{VH} - \epsilon_F)^2} + \epsilon_F$ . Here the sign in the prefactor of the square root is the same as the sign of  $\epsilon_{VH} - \epsilon_F$ . In order to get a consistent explanation to the spectrum, we assume that the tube is hole doped (i.e.,  $\epsilon_F < 0$ ) and that the positive voltage corresponds to the negative electron energy.

It is interesting that peak 2 is broader than peak 3. This indicates that peak 2 corresponds to two overlapped peaks: one is a superconducting quasi-particle peak and another is a Van Hove singularity located slightly above the Fermi level. Peak 3 corresponds to another superconducting quasiparticle peak. From the positions of peak 2, 3, and 4, we deduce that  $\Delta(0) = 54.4$  meV,  $\epsilon_{VH1} = \pm 54.4$  meV,  $\epsilon_{VH2} = \pm 108.5$  meV  $\simeq 2\epsilon_{VH1}$ , and  $\epsilon_F = -55.0$  meV. The positions of Van Hove singularities agree with the theoretical prediction for an armchair tube [51]. With the values of  $\epsilon_{VH1}$ ,  $\epsilon_{VH2}$  and  $\Delta(0)$ , we can predict the other peak positions. For example, we predict  $V_1 = -121.6$  mV and  $V_5 = +121.6$  mV—in excellent agreement with the measured results. Using  $\epsilon_{VH1} = 54.4$  meV,  $d = 17$  nm, and the relation  $\epsilon_{VH1} = 3a_{C-C}\gamma_o/d$  (Ref. [51]), we find that  $\gamma_o = 2.2$  eV, in quantitative agreement with another independent measurement [52].

Since the Fermi level is right on the first Van Hove singularity in this MWNT, the large enhancement in the density of states due to the Van Hove singularity leads to a large increase in the condensation energy, and thus a large suppression of QPS [9]. The observed sharp quasiparticle peak at the gap edge should be related to the substantially reduced QPS. The subgap features in the spectrum may be related to QPS or gap anisotropy. The much lower  $T_{c0}$  in the outermost layer of this MWNT is due to the fact that electron-plasmon coupling is significantly reduced when the second subband is crossed [3].

## 5 Density of states in MWNTs

As discussed above, there are metallic and semiconducting chirality shells that are nested to form MWNTs. Statistically, there should be one-third metallic chirality shells. However, electrical transport measurements on physically separated MWNTs indicate that about 80% of the outermost shells have metallic chiralities [48]. This implies that about 80% of the shells in MWNTs should have metallic chiralities. This conclusion is supported by an independent measurement of electron spin susceptibility using ESR technique [53].

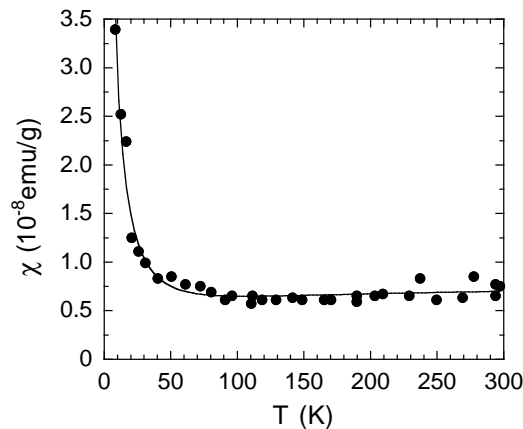


Figure 11: Electron spin susceptibility for a physically separated MWNT film. The data are extracted from Ref. [53].

Fig. 11 shows the temperature dependence of the spin susceptibility for physically separated MWNTs. It is interesting that below about 30 K the spin susceptibility is

dominated by a Curie term ( $\propto 1/T$ ). We can attribute this term to the localized electrons in semiconducting chirality shells because doped semiconducting chirality tubes are shown to be insulating [54]. If the remaining metallic chirality shells are room-temperature superconductors with a minimum superconducting gap  $\Delta_{min}$ , the temperature dependence of the density of states should be proportional to  $\exp(-\Delta_{min}/k_B T)$ . The total susceptibility is then given by

$$\chi_s = \frac{C}{T} + \chi_\infty \exp(-\Delta_{min}/k_B T). \quad (3)$$

The solid line in Fig. 11 is the fitted curve of Eq. 3. One can see that the fit is good. The fitting parameters are  $\chi_\infty = (7.8 \pm 0.8) \times 10^{-9}$  emu/g,  $\Delta_{min} = 6.9 \pm 1.5$  meV, and  $C = (3.97 \pm 0.07) \times 10^{-7}$  emu K/g. From the value of  $\chi_\infty$ , we calculate the normal-state density of states at the Fermi level to be  $2.94 \times 10^{-3}/\text{eV atom}$ . Since the Fermi energy  $\epsilon_F = -55$  meV and the average diameter of the outermost shells is about 10 nm [53], the Fermi level is crossing the first subband of nearly all the metallic shells. Assuming 80% metallic chirality shells and using a theoretical result [51], we find that the density of states  $N(\epsilon_F) = 0.8(2\sqrt{3}/\pi^2)(1/\gamma_o)(a_{C-C}/\bar{d})$ , where  $\bar{d}$  is a diameter averaged for all the shells,  $a_{C-C} = 0.142$  nm and  $\gamma_o = 2.2$  eV. If we take the average diameter of the innermost shells to be 2 nm and the average diameter of the outermost shells to be 10 nm (Ref. [53]), then  $\bar{d} = 6$  nm. Substituting  $\bar{d} = 6$  nm into the above equation yields  $N(\epsilon_F) = 2.86 \times 10^{-3}/\text{eV atom}$ , in excellent agreement with that deduced from Fig. 11. Moreover, the carrier density is  $-\epsilon_F N(\epsilon_F) = 1.6 \times 10^{-4}/\text{atom} = 1.6 \times 10^{19}/\text{cm}^3$ , in remarkably good agreement with the measured one ( $1.6 \times 10^{19}/\text{cm}^3$ ) [45].

## 6 Meissner effect and Remnant Magnetization in MWNTs

It is well known that the diamagnetic susceptibility of graphite is very small when the magnetic field is along the plane. It is also shown that the diamagnetic susceptibility is small when the field is along the tube axis direction. If we take  $d = 6$  nm and  $\epsilon_F = -55$  meV (see above) and use the theoretically calculated result of Ref. [55], we estimate  $\chi_{||}(0) \simeq -1.7 \times 10^{-6}$  emu/g, which is a factor of 7 smaller than the measured one ( $-1.1 \times 10^{-5}$  emu/g) [53]. This large discrepancy can be naturally resolved if the MWNTs are superconductors that contribute to diamagnetism due to the Meissner effect.

For tubes of radius  $r$  with magnetic field parallel to the tube axis direction, the zero-temperature diamagnetic susceptibility due to the Meissner effect is given by

$$\chi_{||}(0) = -\frac{\bar{r}^2}{32\pi\lambda_\theta^2(0)}. \quad (4)$$

Here  $r$  is the radius of tubes,  $\bar{r}^2$  is the average value of  $r^2$ , and  $\lambda_\theta(0)$  is the penetration depth when the screening current is along the circumferential direction. The above equation is valid only if  $\lambda_\theta(0)$  is larger than the maximum radius of tubes. If we assume that the radii of tubes are equally distributed from 0 to 100 Å, we find  $\bar{r}^2 = 6000 \text{ Å}^2$ . With the weight density of  $2.17 \text{ g/cm}^3$  [44] and  $\chi_{||}(0) = -0.93 \times 10^{-5}$  emu/g [53] (we have subtracted the normal-state diamagnetic susceptibility), we calculate  $\lambda_\theta(0) \simeq 1724 \text{ Å}$ . This value of the penetration depth corresponds to  $n/m_\theta^* = 0.96 \times 10^{21}/\text{cm}^3 m_e$ , where  $m_\theta^*$  is the effective mass of carriers along the circumferential direction. With  $n = 1.6 \times 10^{19}/\text{cm}^3$  (Ref. [45]), we find that  $m_\theta^* \simeq 0.017 m_e$ , which is larger than the in-plane effective mass of  $0.012 m_e$  for graphites [56]. Since the effective mass along the tube axis direction is nearly zero [54], the value of  $m_\theta^*$  indicates that MWNTs are quasi-1D superconductors.

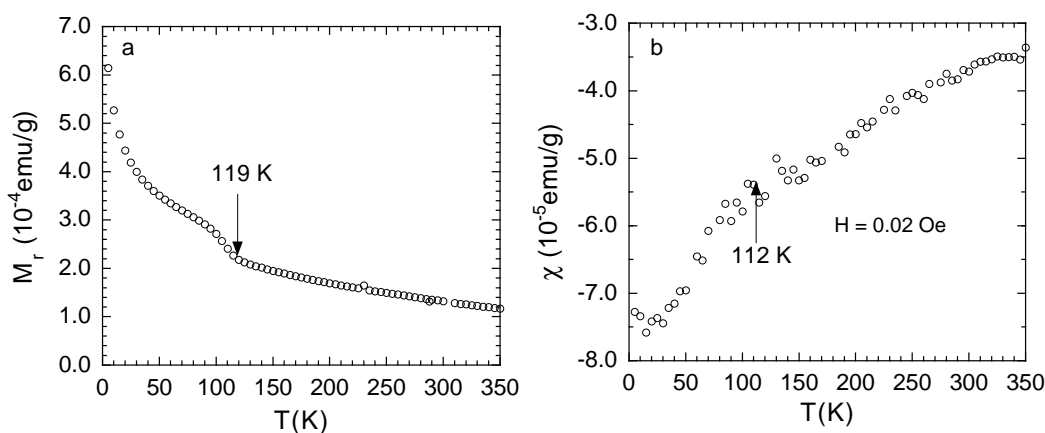


Figure 12: a) Temperature dependence of the remnant magnetization for multi-walled nanotubes. b) The field-cooled susceptibility as a function of temperature in a field of 0.020 Oe. After Ref. [7].

From Eq. 4, we can see that  $\chi_{\parallel}(0)$  will increase linearly with increasing  $r^2$ . For Josephson coupled MWNT bundles in unprocessed ropes, the effective  $r^2$  is much larger than that for physically separated MWNTs. This can naturally explain why the total low-temperature diamagnetic susceptibility for unprocessed MWNTs is larger than that for physically separated MWNTs by a factor of 4.3 (see the result of Ref. [53]). Without superconductivity in these MWNTs, it is very difficult to account for such a large enhancement in the diamagnetic susceptibility for the physically coupled MWNTs.

To further show that MWNTs are room-temperature superconductors, we show in Fig. 12 the temperature dependencies of the remnant magnetization  $M_r$  and the diamagnetic susceptibility for our MWNT ropes. It is apparent that the temperature dependence of  $M_r$  (Fig. 12a) is similar to that of the diamagnetic susceptibility (Fig. 12b) except for the opposite signs. This behavior is expected for a superconductor. Although the  $M_r$  was also observed by Tsebro *et al.* up to 300 K [57], the observation of  $M_r$  alone does not give unambiguous evidence for RT superconductivity since such a  $M_r$  could be caused by ferromagnetic impurities.

We now rule out the existence of ferromagnetic impurities. If there were ferromagnetic impurities, the total susceptibility would tend to turn up below 120 K where the  $M_r$  increases suddenly. This is because paramagnetic susceptibility and  $M_r$  should increase simultaneously for ferromagnetic impurities. In contrast, the susceptibility suddenly turns down rather than turns up below 120 K (Fig. 12b). This provides strong evidence that the observed  $M_r$  in our MWNTs are not associated with the presence of random ferromagnetic impurities but with superconductivity. Moreover, the large anisotropy in the  $M_r$  of a MWNT rope [57] suggests that this  $M_r$  is unlikely to arise from random magnetic impurities, because such an effect should be isotropic with respect to the field orientation.

## 7 Conclusion

Although we may feel that RT superconductivity in carbon nanotubes is too wonderful to believe, we find that the over twenty arguments from Refs. [7-11] and herein are too compelling to be false. The mechanism for RT superconductivity may arise from strong electron-phonon and electron-plasmon coupling in the quasi-1D electronic systems [3].

**Acknowledgment:** I thank Dr. Pieder Beeli for his valuable comments.

\*Correspondence should be addressed to gzhao2@calstatela.edu.

## References

- [1] W. L. McMillan, Phys. Rev. **167**, 331 (1968).
- [2] A. S. Alexandrov and N. F. Mott, *Polarons and Bipolarons* (World Scientific, Singapore, 1995).
- [3] Y.C. Lee and B. S. Mendoza, Phys. Rev. B **39**, 4776 (1989).
- [4] S. M. Cui and C. H. Tsai, Phys. Rev. B **44**, 12500 (1991).
- [5] R. Saito *et al.*, Appl. Phys. Lett. **60**, 2204 (1992).
- [6] H. Ajiki and T. Ando, J. Phys. Soc. Jpn. **62**, 1255 (1992).
- [7] G. M. Zhao and Y. S. Wang, cond-mat/0111268.
- [8] G. M. Zhao, cond-mat/0208197.
- [9] G. M. Zhao, cond-mat/0208198.
- [10] G. M. Zhao, cond-mat/0208200.
- [11] G. M. Zhao, cond-mat/0208201.
- [12] T. Giamarchi and H. J. Schulz, Phys. Rev. B **37**, 325 (1988).
- [13] E. Orignac and T. Giamarchi, Phys. Rev. B **56**, 7167 (1997).
- [14] A. A. Abrikosov and J. A. Rhyzkin, Adv. Phys. **27**, 147 (1978).
- [15] N. Giordano, Phys. Rev. B **41**, 6350 (1990).
- [16] A. D. Zaikin *et al.*, Phys. Rev. Lett. **78**, 1552 (1997).
- [17] N. Giordano and E. R. Schuler, Phys. Rev. Lett. **63**, 2417 (1989).
- [18] N. Giordano, Phys. Rev. B **43**, 160 (1991).
- [19] A. Bezryadin, C. N. Lau, and M. Tinkham, Nature (London) **404**, 971 (2000).
- [20] H. T. Soh *et al.*, Appl. Phys. Lett. **75**, 627 (1999).
- [21] Z. Yao, C. L. Kane, and C. Dekker, Phys. Rev. Lett. **84**, 2941 (2000).
- [22] A. Bachtold *et al.*, Phys. Rev. Lett. **84**, 6082 (2000).
- [23] P. J. de Pablo *et al.*, Appl. Phys. Lett. **74**, 323 (1999).
- [24] Z. K. Tang *et al.*, Science, **292**, 2462 (2001).
- [25] A. Komnik and R. Egger, cond-mat/9906150 (1999).
- [26] C. Kane, L. Balents, and M. P. A. Fisher, Phys. Rev. Lett. **79**, 5086 (1997).

- [27] R. Tarkiainen *et al.*, Phys. Rev. B **64**, 195412 (2001).
- [28] J. Kong *et al.*, Phys. Rev. Lett. **87**, 106801 (2001).
- [29] J. W. G. Wildoer *et al.*, Nature (London) **391**, 59 (1998).
- [30] R. S. Lee *et al.*, Nature (London) **388**, 255 (1997).
- [31] G. D. Mahan and G. S. Canright, Phys. Rev. B **35**, 4365 (1987).
- [32] M. Kociak *et al.*, Phys. Rev. Lett. **86**, 2416 (2001).
- [33] M. Ouyang *et al.*, Science **292**, 702 (2001).
- [34] R. Walter *et al.*, Bull Am. Phys. Soc. **47**, 361 (2002).
- [35] M. Krantz *et al.*, Phys. Rev. B **38**, 4992 (1988).
- [36] B. Friel, C. Thomsen, and M. Cardona, Phys. Rev. Lett. **65**, 915 (1990).
- [37] K. M. Ham, *et al.*, Phys. Rev. B **47**, 11 439 (1993).
- [38] R. Zeyher and G. Zwicknagl, Z. Phys. B **78**, 175 (1990).
- [39] R. Zeyher and G. Zwicknagl, Solid State Commun. **66**, 617 (1988).
- [40] M. Tinkham, *Introduction to Superconductivity* (McGraw-Hill, 1996).
- [41] S. Frank *et al.*, Science **280**, 1744 (1998).
- [42] P. Poncharal *et al.*, J. Phys. Chem. B **106**, 12104 (2002).
- [43] T. W. Ebbesen *et al.*, Nature (London) **382**, 54 (1996).
- [44] D. Qian *et al.*, Appl. Phys. Lett. **76**, 2828 (2000).
- [45] G. Baumgartner *et al.*, Phys. Rev. B **55**, 6704 (1997).
- [46] G. T. Kim *et al.*, Phys. Rev. B **58**, 16 064 (1998).
- [47] V. B. Geshkenbein, L. B. Ioffe, and A. J. Millis, Phys. Rev. Lett. **80**, 5778 (1998).
- [48] C. Schönenberger *et al.*, Appl. Phys. A **69**, 283 (1999).
- [49] Y.-K. Kwon and D. Tomanek, Phys. Rev. B **58**, R16001 (1998).
- [50] S. Sanvito *et al.*, Phys. Rev. Lett. **84**, 1974 (2000).
- [51] J. W. Mintmire and C. T. White, Phys. Rev. Lett. **81**, 2506 (1998).
- [52] P. G. Collins, M. S. Arnold, P. Avouris, Science **292**, 706 (2001).
- [53] O. Chauvet *et al.*, Phys. Rev. B **52**, R6963 (1995). The aligned nanotube films were produced by a process in which the tubes are ultrasonically separated.
- [54] P. L. McEuen *et al.*, Phys. Rev. Lett. **83**, 5098 (1999).
- [55] J. P. Lu, Phys. Rev. Lett. **74**, 1153 (1995).
- [56] V. Bayot *et al.*, Phys. Rev. B **40**, 3514 (1989).
- [57] V. I. Tsebro, O. E. Omelyanovskii, and A. P. Moravskii, JETP Lett. **70**, 462 (1999).